Di X, Biswal BB. 2014. Modulatory interactions between the default mode network and task positive networks in resting-state. PeerJ 2:e367 https://doi.org/10.7717/peerj.367

Modulatory Interactions between the Default Mode Network and Task Positive Networks in Resting-State

Communications between different brain systems are critical to support complex brain functions. Unlike generally high functional connectivity between brain regions from same system, functional connectivity between regions from different systems are more variable. In the present study, we examined whether the connectivity between different brain networks were modulated by other regions by using physiophysiological interaction (PPI) on resting-state functional magnetic resonance imaging data. Spatial independent component analysis was first conducted to identify the default mode network (DMN) and several task positive networks, including the salience, dorsal attention, left and right executive networks. PPI analysis was conducted between pairs of these networks to identify networks or regions that showed modulatory interactions with the two networks. Network-wise analysis revealed reciprocal modulatory interactions between the DMN, salience, and executive networks. Together with the anatomical properties of the salience network regions, the results suggest that the salience network may modulate the relationship between the DMN and executive networks. In addition, voxel-wise analysis demonstrated that the basal ganglia and thalamus positively interacted with the salience network and the dorsal attention network, and negatively interacted with the salience network and the DMN. The results demonstrated complex relationships among brain networks in resting-state, and suggested that between network communications of these networks may be modulated by some critical brain structures such as the salience network, basal ganglia, and thalamus.

PeerJ PrePrints | https://peerj.com/preprints/124v1/ | v1 received: 27 Nov 2013, published: 27 Nov 2013, doi: 10.7287/peerj.preprints.124v1

Modulatory Interactions between the Default Mode Network and Task Positive Networks in Resting-State

Xin Di, Bharat B. Biswal*

Department of Biomedical Engineering, New Jersey Institute of Technology, Newark, NJ, 07102, USA.

*Corresponding author:
Bharat B. Biswal, PhD
607 Fenster Hall, University Height
Newark, NJ, 07102, USA
bbiswal@yahoo.com

Introduction

The human brain is intrinsically organized as different networks as generally revealed by resting-state functional magnetic resonance imaging (fMRI) (Beckmann et al. 2005; Golland et al. 2008; Yeo et al. 2011). Brain regions within a network generally convey relatively higher connectivity than regions from different networks (Biswal et al. 1995; Cordes et al. 2000; Greicius et al. 2003), thus constitute modular organizations of brain functions (Doucet et al. 2011; Meunier et al. 2009; Salvador et al. 2005). On the other hand, brain regions that belonged to different networks generally have smaller connectivity, however, between network communications are considered to be critical to support complex brain functions which need to integrate resources from different brain systems (Bullmore and Sporns 2012; Cole et al. 2013).

There are roughly two big systems in the brain, one showed consistent activation across different tasks (i.e. task positive network, (Shulman et al. 1997a)), while the other showed consistent deactivation (i.e. default mode network, DMN, (Shulman et al. 1997b)). These two systems revealed moment to moment anticorrelation even when one wasn't performing explicit tasks (Fox et al. 2005). The negative correlation between the DMN and the task positive network is developed in adolescence (Chai et al. 2013), and may serve as a suppression mechanism that inhibits unwanted noises, thus make behavior responses more reliable (Anticevic et al. 2012; Kelly et al. 2008; Spreng et al. 2010; Wen et al. 2013). Although the original paper of anticorrelation has been questioned because of global regression in data processing (Murphy et al. 2009), further studies have shown that the negative correlation between the DMN and the task positive network still presents without global regression (Chai et al. 2012; Fox et al. 2009), and has its neuronal origins (Keller et al. 2013). However, the controversies of negative correlation may partially due to the fact that the connectivity between the DMN and the task positive network is highly variable (Chang and Glover 2010; Kang et al. 2011).

The negative connectivity between the task positive network and DMN has been shown to be modulated or mediated by other networks, which may provide hints on the variability of the negative correlation. Sridharan and colleagues showed that the salience network (Seeley et al. 2007) activated the executive network which is part of the task positive network, and deactivated the DMN during both task performing conditions and resting-state (Sridharan et al. 2008). In addition, Spreng and colleagues suggested that the relationship between the DMN and dorsal attention network was mediated by the nodes of the frontoparietal control network (Spreng et al. 2013). Thus, the relationship between the DMN and different component of the task positive network, e.g. the salience, dorsal attention, (left and right) executive networks may convey complex interactions among each others. In the present study, we aimed to study whether the relationship between two networks is modulated by other networks or regions by using physiophysiological interaction (PPI) (Di and Biswal 2013a; Friston et al. 1997), which may provide a novel revenue to characterize the complex relationships among these networks.

Specifically, we sought to systematically investigate the modulatory interaction between the DMN and other task positive networks using PPI analysis on resting-state fMRI data. Spatial independent component analysis (ICA) was first performed to identify the networks of interest, including the DMN, salience, dorsal attention, left executive, and right executive networks. PPI analysis was then performed between each two of networks with other networks or with all other brain regions. This between network PPI analysis aimed to identify networks or regions that modulate the dynamic relationship between the two predefined networks. Based on notion that the salience network played an important role in switching of large scale brain networks (Menon and Uddin 2010; Sridharan et al. 2008), we predict that the salience network may show interaction effects with the DMN and executive networks.

Methods

Subjects

The resting-state fMRI data was derived from the Beijing_Zang dataset of the 1000 functional connectomes project (http://fcon_1000.projects.nitrc.org/) (Biswal et al. 2010). This dataset organically contains 198 subjects. The first 64 subjects without large head motion were included in the current analysis (40 female/ 24 male). The mean age of these subjects was 21.1 years (range from 18 to 26 years).

Scanning parameters

The MRI data were acquired using a SIEMENS Trio 3-Tesla scanner from Beijing Normal University. 230 resting-state functional data were acquired for each subject using TR of 2 s. The resolution of the fMRI images was 3.125 x 3.125 x 3 mm with 64 x 64 x 36 voxels. The T1-weighted sagittal three-dimensional magnetization-prepared rapid gradient echo (MP-RAGE) sequence was acquired using the following parameters: 128 slices, TR = 2530 ms, TE = 3.39 ms, slice thickness = 1.33 mm, flip angle = 7°, inversion time = 1100 ms, FOV = 256 × 256 mm^2.

Functional MRI data analysis

Preprocessing

The fMRI image preprocessing and analysis were conducted using SPM8 package (http://www.fil.ion.ucl.ac.uk/spm/) under MATLAB 7.6 environment (http://www.mathworks.com). For each subject, the first two functional images were discarded, resulting in 228 images for each subject. The functional images were motion corrected, and coregistered to subject's own high resolution anatomical image. Next, subject's anatomical images were normalized to the T1 template provided by SPM package in MNI space (Montreal Neurological Institute). Then, the normalization parameters were used to normalize all the functional images into MNI space, and the functional images were resampled into 3 x 3 x 3 mm^3 voxels. Finally, all the functional images were smoothed using a Gaussian kernel with 8 mm full width at half maximum (FWHM).

Spatial ICA

Spatial ICA was conducted to define networks for the PPI analysis using the Group ICA of fMRI Toolbox (GIFT) (http://icatb.sourceforge.net/) (Calhoun et al. 2001). Twenty components were extracted. The DMN, salience, dorsal attention, left executive, and right executive networks were visually identified according to Cole and colleagues (Cole et al. 2010) (Figure 1). Time series associated with these five components were obtained for each subject for following PPI analysis. To aid interpretation of the PPI results, simple correlations among the five networks were calculated for each subject. The correlation values were transformed into Fisher's z, and statistical significance were tested across subjects using one sample t-test.

[Insert Figure 1 here]

PPI analysis

Physiophysiological interaction analysis, along with its variant psychophysiological interaction, were first proposed by Friston and colleagues to characterize modulated connectivity by another region or a psychological manipulation (Friston et al. 1997). The present analysis focused on the modulation of connectivity by other regions or networks. Specifically, time series of two networks were used to define an interaction model using a linear regression framework.

$$y = \beta_{N1} \cdot x_{N1} + \beta_{N2} \cdot x_{N2} + \beta_{PPI} \cdot x_{N1} \cdot x_{N2} + \varepsilon$$

Where x_{N1} and x_{N2} represent the time series of two networks. Critically, we are interested in whether the interaction term of the two time series is correlated with the time series of a given voxel or region y (the effect of β_{PPI}). A positive interaction effect implies that the connectivity between the resultant region and one of the network is positively modulated by the other network. While a negative interaction effect implies that the connectivity between the resultant region and one of the network is negatively modulated by the other network. In practice, the time series of the two networks were deconvolved with hemodynamic response function (hrf), so that the PPI term was calculated in the neuronal level but not hemodynamic level (Gitelman et al. 2003).

Before PPI analysis, the time series of each network were preprocessed in following steps. Six rigid-body motion parameters, the first principle component time series of white matter (WM) signal, and the first principle component time series of cerebrospinal fluid (CSF) signal were regressed out from the original time series by using linear regression model. The subject specific WM and CSF masks were derived from their own segmented WM and CSF images, with a threshold of 0.99 to make sure that GM voxels were excluded from the masks. Next, a high-pass filter of 0.01 Hz was applied on the time series to minimize low frequency scanner drift. The preprocessed time series of two networks were first deconvolved with the hrf using a simple empirical Bayes procedure, so that the resulting time course represented an approximation to neural activity (Gitelman et al. 2003). Next, the two neural time series were detrended and point multiplied, so that the resulting time series represented the interaction of neural activity between two networks. And lastly, the interaction time series was convolved with the hrf, resulting in an interaction variable in BOLD level. The PPI terms were calculated for each pair of the five networks.

Network-wise PPI analysis was first conducted to directly examine the relationships among networks, which is similar to von Kriegstein and Giraud (von Kriegstein and Giraud 2006). In the network-wise analysis, the dependent variable is the time series of a network rather than the time series of every voxel in the brain. In the PPI linear regression model, the main effects of the two networks, and the PPI effects between them were added as independent variables along with a constant regressor. After model estimation, the beta values corresponding to the PPI effects were used to perform statistics against zero by using one-sample t-test. Critical p values were set as $p < 0.05$ after Bonferroni correction (corresponding to a raw p value of 0.0017 after correcting for totally 30 comparisons).

In addition, voxel-wise PPI analysis was also performed to identify regions across the whole brain that were associated with the PPI effect. The PPI terms were calculated for each pairs of the five networks, resulting in ten separate PPI effects. Then separate PPI models were built for each subject using general linear model (GLM) framework. The GLM model contained two regressors representing the main effects of two ROIs time series, one regressor representing the PPI effect, two regressors representing WM and CSF signals, and six regressors representing head motion effects. An implicit high pass filter of 1/100 Hz was used. For each PPI effect, 2nd-level one sample t-test was conducted to make group-level inference. Simple t contrast of 1 or -1 was defined to reveal positive or negative PPI effects, respectively. The resulting clusters were first height thresholded at $p < 0.001$, and cluster-level false discovery rate (FDR) corrected at $p < 0.05$ based on random field theory (Chumbley and Friston 2009).

Results

Simple correlations among networks

As expected, the DMN showed negative correlations with the salience network (mean Fisher's z -0.299) and the dorsal attention network (mean Fisher's z -0.530). However, the DMN revealed positive correlations with the left executive network (mean Fisher's z 0.184) and the right executive network (mean Fisher's z 0.247). Mean correlations among other networks are listed in Table 1.

[Insert Table 1 here]

Network-wise PPI analysis

All significant network-wise PPI effects were positive (Figure 2). Firstly, positive PPI effects were observed among the salience, DMN, and right executive networks in all of the three ways.

PeerJ PrePrints | https://peerj.com/preprints/124v1/ | v1 received: 27 Nov 2013, published: 27 Nov 2013, doi: 10.7287/peerj.preprints.124v1

The time series of salience network were correlated with the interaction of the DMN and right executive network ($M_{beta} = 0.054; t = 4.09, p = 1.25 x 10^{-4}$). The time series of DMN were correlated with the interaction of the salience and right executive network ($M_{beta} = 0.060; t = 4.77, p = 1.14 x 10^{-5}$). And the time series of the right executive network were correlated with the interaction of the salience network and DMN ($M_{beta} = 0.109; t = 8.27, p = 1.19 x 10^{-11}$). In addition, the left executive time series were also correlated with the interaction of the salience network and DMN ($M_{beta} = 0.048; t = 3.67, p = 4.98 x 10^{-4}$). Secondly, positive PPI effects were also observed among the salience and bilateral executive networks. The left executive network time series were correlated with the interaction of the salience and right executive network ($M_{beta} = 0.046; t = 4.01, p = 1.65 x 10^{-4}$), and the right executive network times series were correlated with the interaction of the salience and left executive network ($M_{beta} = 0.053; t = 3.94, p = 2.06 x 10^{-4}$). Lastly, positive PPI effects were also observed among the dorsal attention, and bilateral executive networks, i.e. the right executive network time series were correlated with the interaction effects of the dorsal attention and left executive networks ($M_{beta} = 0.058; t = 4.31, p = 5.91 x 10^{-5}$).

[Insert Figure 2 here]

Voxel-wise PPI analysis

As shown in Figure 3 and Table S1, regions that revealed positive modulatory interaction with the DMN and the salience network resemble a typical task positive network. These regions included the bilateral dorsolateral prefrontal cortex, bilateral parietal lobule, bilateral middle temporal gyrus, and two small clusters in the precuneus and posterior cingulate cortex. In contrast, several regions showed negative moduloatory interaction, including the cigulate gyrus, bilateral putamen, right insula, precuneus, and paracentral lobule.

[Insert Figure 3 here]

The PPI results of the DMN and other task positive networks are shown in Figure 4. A typical fronto-parietal network regions showed positive modulatory interactions with the DMN and the dorsal attention network (Figure 4A), including the left middle frontal gyrus, bilateral parietal lobule, bilateral superior frontal gyrus, and left superior temporal gyrus (see also Table S2). In contrast, one region in the inferior parietal lobule revealed negative modulatory interaction with the DMN and the dorsal attention network. Only one region located in the right inferior parietal lobule revealed negative modulatory interaction with the DMN and the left executive network (Figure 4B and Table S3). No positive effects were observed. For the modulatory interactions of the DMN and right executive network (Figure 4C), positive effects were observed in the bilateral insula, cingulate gyrus, right inferior parietal lobule, bilateral middle frontal gyrus, anterior cingulate cortex, and right thalamus (see also Table S4). Negtive effects were observed in the right superior and middle frontal gyrus.

[Insert Figure 4 here]

The PPI results of the salience and other task positive networks are illustrated in Figure 5. For the modulatory interactions of the salience network and the dorsal attention network (Figure 5A), positive effects were observed in the medial frontal gyrus, subcortical nucleus including right thalamus, bilateral claustrum, and right lentiform nucleus, and bilateral parietal lobule (see also Table S5). Negative effects were observed in the left middle and inferior frontal gyrus. For the modulatory interactions of the salience network and the left executive network (Figure 5B), positive PPI effects were observed in the medial frontal tyrus, left superior temporal gyrus, left middle frontal gyrus, and left middle temporal gyrus (see also Table S6). Negative effects were observed in the left insula. For the modulatory interactions of the salience network and the right executive network (Figure 5C), positive effects were observed in the superior frontal gyrus, bilateral inferior frontal gyrus, bilateral superior temporal gyrus, right precentral and postcentral gyrus (see also Table S7). No negative PPI effects were observed.

[Insert Figure 5 here]

The PPI results among other positive networks were shown in Figure 6. For the modulatory interactions of the dorsal attention network and the left executive network (Figure 6A), positive effects were observed in the left inferior parietal lobule, left middle frontal gyrus, and right cerebellum (see also Table S8). No negative effects were observed. For the modulatory interactions of the dorsal attention network and the right executive network (Figure 6B), positive effects were observed in the right middle temporal gyrus and right precuneus (see also Table S9). No negative effects were observed. Lastly, for the modulatory interactions of the left and right executive networks (Figure 6C), positive PPI effects were observed in the bilateral precuneus, right inferior parietal lobule, left cerebellum (see also Table S10). Negative effects were observed in the left superior frontal gyrus.

[Insert Figure 6 here]

Discussion

Similar to previous studies, we observed negative correlations between the DMN and some task positive networks, for example the salience and dorsal attention networks. However, the DMN revealed small but consistent positive correlations with both the left and right executive networks. These results suggested that the DMN revealed complex relationships with different components of task positive networks. It should be noted that the correlation values are subjective to preprocessing steps and level of noises (Fox et al. 2009; Saad et al. 2012; Weissenbacher et al. 2009), so that the absolute values of correlations cannot be treated seriously. Instead, we focused on modulatory interactions which are less likely to be affected by noises, and observed positive modulatory interactions between the DMN, the salience network and the executive networks. Specifically, network-wise analysis revealed reciprocally positive modulatory interactions among the DMN, the salience, and the right executive networks. These effects can also be observed in the voxel-wise analysis. For example, the analysis of the DMN and the salience network revealed clusters that assemble the bilateral executive network (Figure 3). The analysis of the DMN and right executive network revealed clusters that assemble the salience network (Figure 4C). Lastly, the analysis of the salience network and the right executive network revealed clusters that were part of the DMN (Figure 5C). The left executive network also showed association with the interaction of the DMN and the salience network in both PPI-wise and voxel-wise analysis (Figure 2 and 3). These results are consistent with our recent findings that the connectivity between the DMN and frontoparietal regions is positively modulated by the salience network activity (Di and Biswal 2013b). The convergent results suggested complex modulatory effects among the DMN, salience, and executive networks.

Among the DMN, salience, and executive networks, the salience network may play a critical role due to its anatomical connections and causal influences. Anatomically, the salience network contains a special type of neuron termed von Economo neuron (Allman et al. 2010), which are spindle like bipolar neurons with thick axons. These properties enable von Economo neurons to rapidly pass information from the salience network regions to other brain regions, which might be vital for the emergence of social behaviors (Butti et al. 2009). A recent study has demonstrated that the regions containing von Economo neurons had functional connectivity with both the DMN and frontoparietal networks (Cauda et al. 2013). In terms of causal influence, studies using Granger causality analysis suggested that the salience network sent information to both the DMN and executive networks (Deshpande et al. 2011; Liao et al. 2010; Sridharan et al. 2008; Yan and He 2011). Taken together, it is possible that the salience network, in addition to activate the executive network and deactivate the DMN (Sridharan et al. 2008), directly modulate the relationship between the executive network and DMN.

The modulation may reflect that saliency signals conveyed by the salience network increase the communication between the executive system and internal oriented system.

PeerJ PrePrints | https://peerj.com/preprints/124v1/ | v1 received: 27 Nov 2013, published: 27 Nov 2013, doi: 10.7287/peerj.preprints.124v1

Alternatively, because the absolute connectivity between the executive network and the DMN is subject to preprocessing steps, and these two networks are generally considered as anticorrelated (Chai et al. 2012; Fox et al. 2005; Keller et al. 2013), it is also possible that the modulation may reflect decreased anticorrelation between the DMN and executive networks. The decreased anticorrelation might suggest an absence of modulation of top-down signals from the DMN to central executive regions (Anticevic et al. 2012). In line with this notion, impaired salience network functions in patients of schizophrenia is coincidentally associated with altered connectivity between the executive network and DMN (Manoliu et al. 2013a; Manoliu et al. 2013b). The modulatory model of the salience network on the executive network and DMN may provide novel avenue to understand dysfunctions of network communications in patients with schizophrenia (Menon 2011).

In addition to the modulatory interactions between the DMN and task positive networks, we also observed modulatory interactions among different task positive networks. These interactions were mainly among the salience network and bilateral executive networks, and among the dorsal attention network and bilateral executive networks. The frontoparietal executive network is generally identified bilaterally when using seed-based correlations and cluster analysis (Dosenbach et al. 2007; Yeo et al. 2011), however, separate left and right lateralized frontopareital networks can be reliably identified when using ICA (Beckmann et al. 2005; Biswal et al. 2010). The current analysis revealed a moderate correlation between the left and right executive networks (mean Fisher's z 0.43), which was the largest correlation among task positive networks. In addition, the modulatory interactions results suggested that the relationship between the left and right frontoparietal networks may be modulated by the salience network and the dorsal attention network. Even thought the left and right frontopareital networks are symmetrically aligned, these two networks are associated with different cognitive functions, with the left executive network more associated with language cognition, and the right counterpart more related to action inhibition and pain perception (Smith et al. 2009). The increased connectivity between the bilateral networks may reflect the increased communication of resources from different executive systems.

Voxel-wise analysis also identified subcortical regions that revealed modulatory interactions with different networks, notably the thalamus and basal ganglia. Specifically, the basal ganglia revealed a negative modulatory interaction with the DMN and salience network (Figure 3), while showed a positive modulatory interaction with the salience and dorsal attention networks (Figure 5A). The basal ganglia is functionally connected to widely distributed cortical regions (Di Martino et al. 2008) via different white matter fibers (Leh et al. 2007; Lehéricy et al. 2004). Models of basal ganglia function have suggested it to be a moderator that modulate connectivity from frontal regions to posterior visual areas to support task switching and attention shifting (den Ouden et al. 2010; van Schouwenburg et al. 2010; Stephan et al. 2008). The current results extended these notion into resting-state, suggesting a general modulating role of the basal ganglia on connectivity between brain networks. In addition, the thalamus revealed positive modulatory interactions with the salience network and dorsal attention network. The thalamus is a critical subcortical structure involving attention (Haynes et al. 2005; O'Connor et al. 2002). It is possible that the salience signal from the salience network enhance the connectivity from the thalamus to the dorsal attention network to allocate attention recourses to the specific stimulus (Fan et al. 2005). Alternatively, the salience signal might modulated top-down connectivity from the dorsal attention network to the thalamus, that facilitate attentional gating of the salient event (Fischer and Whitney 2012; McAlonan et al. 2008; McAlonan et al. 2000). Further studies using causal models are needed to further clarify the dynamic relationships among the thalamus, the salience network, and the dorsal attention network (Di and Biswal 2013c; Friston et al. 2003).

By applying PPI technique to brain networks in resting-state, the current study demonstrated modulatory interactions among different brain systems. Compared with our

PeerJ PrePrints | https://peerj.com/preprints/124v1/ | v1 received: 27 Nov 2013, published: 27 Nov 2013, doi: 10.7287/peerj.preprints.124v1

previous study that examined PPI effects of two regions within the same network (Di and Biswal 2013a), the current results generally revealed larger spatial extent of significant effects. This suggests that the modulatory interaction effects may generally take place in modulation of communications between different brain systems rather than within one system. This notion is in line with the economic theory of brain organization that between module connectivity are more likely to be modulated upon task demands to facilitate brain network reconfigurations (Bullmore and Sporns 2012; Di et al. 2013). However, the spatial distribution of modulatory interaction effects and their functional significance are still open questions, and warrant further explorations.

References

Allman JM, Tetreault NA, Hakeem AY, et al. (2010) The von Economo neurons in frontoinsular and anterior cingulate cortex in great apes and humans. Brain Struct Funct 214:495–517. doi: 10.1007/s00429-010-0254-0

Anticevic A, Cole MW, Murray JD, et al. (2012) The Role of Default Network Deactivation in Cognition and Disease. Trends Cogn Sci. doi: 10.1016/j.tics.2012.10.008

Beckmann CF, DeLuca M, Devlin JT, Smith SM (2005) Investigations into resting-state connectivity using independent component analysis. Philos Trans R Soc Lond B Biol Sci 360:1001–13. doi: 10.1098/rstb.2005.1634

Biswal B, Yetkin FZ, Haughton VM, Hyde JS (1995) Functional connectivity in the motor cortex of resting human brain using echo-planar MRI. Magn Reson Med 34:537–41. doi: 10.1002/mrm.1910340409

Biswal BB, Mennes M, Zuo X-N, et al. (2010) Toward discovery science of human brain function. Proc Natl Acad Sci U S A 107:4734–9. doi: 10.1073/pnas.0911855107

Bullmore E, Sporns O (2012) The economy of brain network organization. Nat Rev Neurosci 13:336–349. doi: 10.1038/nrn3214

Butti C, Sherwood CC, Hakeem AY, et al. (2009) Total number and volume of Von Economo neurons in the cerebral cortex of cetaceans. J Comp Neurol 515:243–59. doi: 10.1002/cne.22055

Calhoun VD, Adali T, Pearlson GD, Pekar JJ (2001) A method for making group inferences from functional MRI data using independent component analysis. Hum Brain Mapp 14:140–51.

Cauda F, Torta DME, Sacco K, et al. (2013) Functional anatomy of cortical areas characterized by Von Economo neurons. Brain Struct Funct 218:1–20. doi: 10.1007/s00429-012-0382-9

Chai XJ, Castañón AN, Ongür D, Whitfield-Gabrieli S (2012) Anticorrelations in resting state networks without global signal regression. Neuroimage 59:1420–8. doi: 10.1016/j.neuroimage.2011.08.048

Chai XJ, Ofen N, Gabrieli JDE, Whitfield-Gabrieli S (2013) Selective Development of Anticorrelated Networks in the Intrinsic Functional Organization of the Human Brain.

Chang C, Glover GH (2010) Time-frequency dynamics of resting-state brain connectivity measured with fMRI. Neuroimage 50:81–98. doi: 10.1016/j.neuroimage.2009.12.011

Chumbley JR, Friston KJ (2009) False discovery rate revisited: FDR and topological inference using Gaussian random fields. Neuroimage 44:62–70. doi: 10.1016/j.neuroimage.2008.05.021

Cole DM, Smith SM, Beckmann CF (2010) Advances and pitfalls in the analysis and interpretation of resting-state FMRI data. Front Syst Neurosci 4:8. doi: 10.3389/fnsys.2010.00008

Cole MW, Reynolds JR, Power JD, et al. (2013) Multi-task connectivity reveals flexible hubs for adaptive task control. Nat Neurosci. doi: 10.1038/nn.3470

Cordes D, Haughton VM, Arfanakis K, et al. (2000) Mapping functionally related regions of brain with functional connectivity MR imaging. AJNR Am J Neuroradiol 21:1636–44.

Deshpande G, Santhanam P, Hu X (2011) Instantaneous and causal connectivity in resting state brain networks derived from functional MRI data. Neuroimage 54:1043–52. doi: 10.1016/j.neuroimage.2010.09.024

Di X, Biswal BB (2013a) Modulatory interactions of resting-state brain functional connectivity. PLoS One 8:e71163. doi: 10.1371/journal.pone.0071163

Di X, Biswal BB (2013b) Dynamic brain functional connectivity modulated by resting-state networks. Brain Struct Funct. doi: 10.1007/s00429-013-0634-3

Di X, Biswal BB (2013c) Identifying the default mode network structure using dynamic causal modeling on resting-state functional magnetic resonance imaging. Neuroimage. doi: 10.1016/j.neuroimage.2013.07.071

Di X, Gohel S, Kim EH, Biswal BB (2013) Task vs. rest-different network configurations between the coactivation and the resting-state brain networks. Front Hum Neurosci 7:493. doi: 10.3389/fnhum.2013.00493

Dosenbach NUF, Fair DA, Miezin FM, et al. (2007) Distinct brain networks for adaptive and stable task control in humans. Proc Natl Acad Sci U S A 104:11073–8. doi: 10.1073/pnas.0704320104

Doucet G, Naveau M, Petit L, et al. (2011) Brain activity at rest: a multiscale hierarchical functional organization. J Neurophysiol 105:2753–63. doi: 10.1152/jn.00895.2010

Fan J, McCandliss BD, Fossella J, et al. (2005) The activation of attentional networks. Neuroimage 26:471–9. doi: 10.1016/j.neuroimage.2005.02.004

Fischer J, Whitney D (2012) Attention gates visual coding in the human pulvinar. Nat Commun 3:1051. doi: 10.1038/ncomms2054

Fox MD, Snyder AZ, Vincent JL, et al. (2005) The human brain is intrinsically organized into dynamic, anticorrelated functional networks. Proc Natl Acad Sci U S A 102:9673–8.

Fox MD, Zhang D, Snyder AZ, Raichle ME (2009) The global signal and observed anticorrelated resting state brain networks. J Neurophysiol 101:3270–83. doi: 10.1152/jn.90777.2008

Friston KJ, Buechel C, Fink GR, et al. (1997) Psychophysiological and modulatory interactions in neuroimaging. Neuroimage 6:218–29.

Friston KJ, Harrison L, Penny W (2003) Dynamic causal modelling. Neuroimage 19:1273–302.

Gitelman DR, Penny WD, Ashburner J, Friston KJ (2003) Modeling regional and psychophysiologic interactions in fMRI: the importance of hemodynamic deconvolution. Neuroimage 19:200–7.

Golland Y, Golland P, Bentin S, Malach R (2008) Data-driven clustering reveals a fundamental subdivision of the human cortex into two global systems. Neuropsychologia 46:540–53. doi: 10.1016/j.neuropsychologia.2007.10.003

Greicius MD, Krasnow B, Reiss AL, Menon V (2003) Functional connectivity in the resting brain: a network analysis of the default mode hypothesis. Proc Natl Acad Sci U S A 100:253–8.

Haynes J-D, Deichmann R, Rees G (2005) Eye-specific effects of binocular rivalry in the human lateral geniculate nucleus. Nature 438:496–9. doi: 10.1038/nature04169

Kang J, Wang L, Yan C, et al. (2011) Characterizing dynamic functional connectivity in the resting brain using variable parameter regression and Kalman filtering approaches. Neuroimage 56:1222–34. doi: 10.1016/j.neuroimage.2011.03.033

Keller CJ, Bickel S, Honey CJ, et al. (2013) Neurophysiological investigation of spontaneous correlated and anticorrelated fluctuations of the BOLD signal. J Neurosci 33:6333–42. doi: 10.1523/JNEUROSCI.4837-12.2013

Kelly AMC, Uddin LQ, Biswal BB, et al. (2008) Competition between functional brain networks mediates behavioral variability. Neuroimage 39:527–37. doi: 10.1016/j.neuroimage.2007.08.008

Von Kriegstein K, Giraud A-L (2006) Implicit multisensory associations influence voice recognition. PLoS Biol 4:e326. doi: 10.1371/journal.pbio.0040326

Leh SE, Ptito A, Chakravarty MM, Strafella AP (2007) Fronto-striatal connections in the human brain: A probabilistic diffusion tractography study. Neurosci Lett 419:113–118.

Lehéricy S, Ducros M, Van de Moortele P-F, et al. (2004) Diffusion tensor fiber tracking shows distinct corticostriatal circuits in humans. Ann Neurol 55:522–9. doi: 10.1002/ana.20030

Liao W, Mantini D, Zhang Z, et al. (2010) Evaluating the effective connectivity of resting state networks using conditional Granger causality. Biol Cybern 102:57–69.

Manoliu A, Riedl V, Doll A, et al. (2013a) Insular Dysfunction Reflects Altered Between-Network Connectivity and Severity of Negative Symptoms in Schizophrenia during Psychotic Remission. Front Hum Neurosci. doi: 10.3389/fnhum.2013.00216

Manoliu A, Riedl V, Zherdin A, et al. (2013b) Aberrant Dependence of Default Mode/Central Executive Network Interactions on Anterior Insular Salience Network Activity in Schizophrenia. Schizophr Bull sbt037–. doi: 10.1093/schbul/sbt037

Di Martino a, Scheres a, Margulies DS, et al. (2008) Functional connectivity of human striatum: a resting state FMRI study. Cereb Cortex 18:2735–47. doi: 10.1093/cercor/bhn041

McAlonan K, Brown VJ, Bowman EM (2000) Thalamic reticular nucleus activation reflects attentional gating during classical conditioning. J Neurosci 20:8897–901.

McAlonan K, Cavanaugh J, Wurtz RH (2008) Guarding the gateway to cortex with attention in visual thalamus. Nature 456:391–4. doi: 10.1038/nature07382

Menon V (2011) Large-scale brain networks and psychopathology: a unifying triple network model. Trends Cogn Sci 15:483–506. doi: 10.1016/j.tics.2011.08.003

Menon V, Uddin LQ (2010) Saliency, switching, attention and control: a network model of insula function. Brain Struct Funct 214:655–67. doi: 10.1007/s00429-010-0262-0

Meunier D, Achard S, Morcom A, Bullmore E (2009) Age-related changes in modular organization of human brain functional networks. Neuroimage 44:715–23. doi: 10.1016/j.neuroimage.2008.09.062

Murphy K, Birn RM, Handwerker DA, et al. (2009) The impact of global signal regression on resting state correlations: are anti-correlated networks introduced? Neuroimage 44:893–905. doi: 10.1016/j.neuroimage.2008.09.036

O'Connor DH, Fukui MM, Pinsk MA, Kastner S (2002) Attention modulates responses in the human lateral geniculate nucleus. Nat Neurosci 5:1203–9. doi: 10.1038/nn957

Den Ouden HEM, Daunizeau J, Roiser J, et al. (2010) Striatal prediction error modulates cortical coupling. J Neurosci 30:3210–9. doi: 10.1523/JNEUROSCI.4458-09.2010

Saad ZS, Gotts SJ, Murphy K, et al. (2012) Trouble at rest: how correlation patterns and group differences become distorted after global signal regression. Brain Connect 2:25–32. doi: 10.1089/brain.2012.0080

Salvador R, Suckling J, Coleman MR, et al. (2005) Neurophysiological architecture of functional magnetic resonance images of human brain. Cereb Cortex 15:1332–42. doi: 10.1093/cercor/bhi016

Van Schouwenburg MR, den Ouden HEM, Cools R (2010) The human basal ganglia modulate frontal-posterior connectivity during attention shifting. J Neurosci 30:9910–8. doi: 10.1523/JNEUROSCI.1111-10.2010

Seeley WW, Menon V, Schatzberg AF, et al. (2007) Dissociable intrinsic connectivity networks for salience processing and executive control. J Neurosci 27:2349–56. doi: 10.1523/JNEUROSCI.5587-06.2007

Shulman GL, Corbetta M, Buckner RL, et al. (1997a) Common Blood Flow Changes across Visual Tasks: I. Increases in Subcortical Structures and Cerebellum but Not in Nonvisual Cortex. J Cogn Neurosci 9:624–647. doi: 10.1162/jocn.1997.9.5.624

Shulman GL, Fiez JA, Corbetta M, et al. (1997b) Common Blood Flow Changes across Visual Tasks: II. Decreases in Cerebral Cortex. J Cogn Neurosci 9:648–663. doi: 10.1162/jocn.1997.9.5.648

Smith SM, Fox PT, Miller KL, et al. (2009) Correspondence of the brain's functional architecture during activation and rest. Proc Natl Acad Sci U S A 106:13040–5. doi: 10.1073/pnas.0905267106

Spreng RN, Sepulcre J, Turner GR, et al. (2013) Intrinsic architecture underlying the relations among the default, dorsal attention, and frontoparietal control networks of the human brain. J Cogn Neurosci 25:74–86. doi: 10.1162/jocn_a_00281

Spreng RN, Stevens WD, Chamberlain JP, et al. (2010) Default network activity, coupled with the frontoparietal control network, supports goal-directed cognition. Neuroimage 53:303–17. doi: 10.1016/j.neuroimage.2010.06.016

Sridharan D, Levitin DJ, Menon V (2008) A critical role for the right fronto-insular cortex in switching between central-executive and default-mode networks. Proc Natl Acad Sci U S A 105:12569–74. doi: 10.1073/pnas.0800005105

Stephan KE, Kasper L, Harrison LM, et al. (2008) Nonlinear dynamic causal models for fMRI. Neuroimage 42:649–62. doi: 10.1016/j.neuroimage.2008.04.262

Weissenbacher A, Kasess C, Gerstl F, et al. (2009) Correlations and anticorrelations in resting-state functional connectivity MRI: a quantitative comparison of preprocessing strategies. Neuroimage 47:1408–16. doi: 10.1016/j.neuroimage.2009.05.005

Wen X, Liu Y, Yao L, Ding M (2013) Top-down regulation of default mode activity in spatial visual attention. J Neurosci 33:6444–53. doi: 10.1523/JNEUROSCI.4939-12.2013

Yan C, He Y (2011) Driving and driven architectures of directed small-world human brain functional networks. PLoS One 6:e23460. doi: 10.1371/journal.pone.0023460

Yeo BTT, Krienen FM, Sepulcre J, et al. (2011) The organization of the human cerebral cortex estimated by intrinsic functional connectivity. J Neurophysiol 106:1125–65. doi: 10.1152/jn.00338.2011

Figure 1

Resting-state networks identified by spatial ICA.

The time series associated with these networks were used in subsequent PPI analysis. The IC maps were z transformed, and thresholded at z > 1.96.

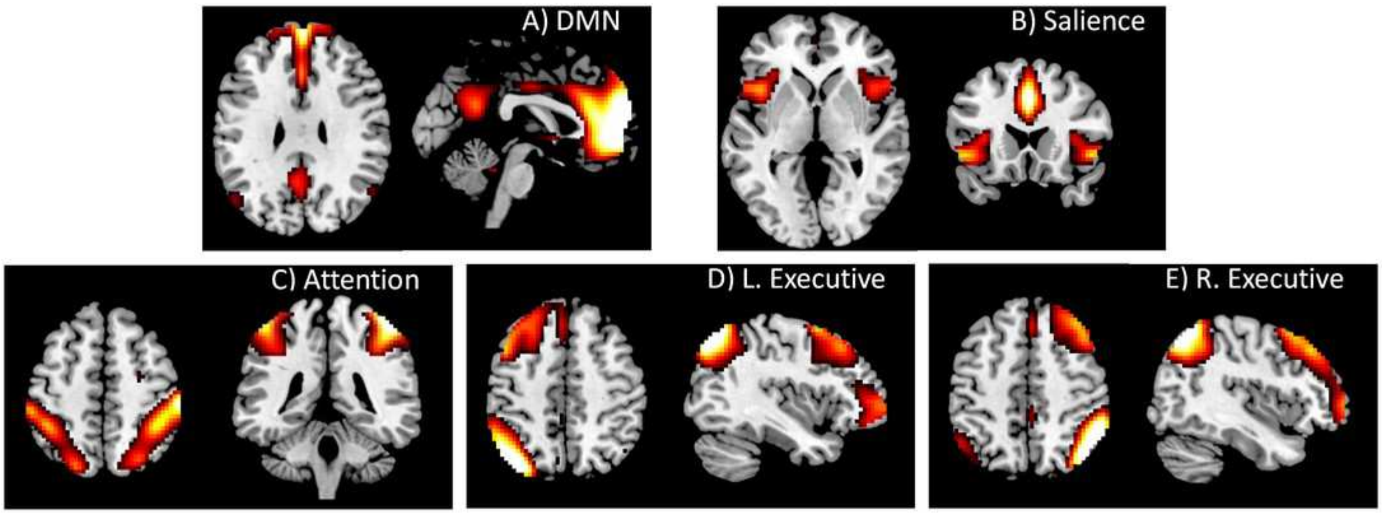

Figure 2

Network-wise PPI results.

Tables indicate the PPI effects between network pairs (row vs. column). Cells outside the tables represent the dependent variables of the time series of different networks (A-E). Arrows and dark gray cell indicate significant PPI effects of a given network (outside cell) and the interaction of two ROIs (cells in the tables). All significant PPI effects are positive. Cells in light gray indicate effects tested but not significant. Statistical significance was determined as $p < 0.05$ after Bonferroni correction of all 30 effects tested.

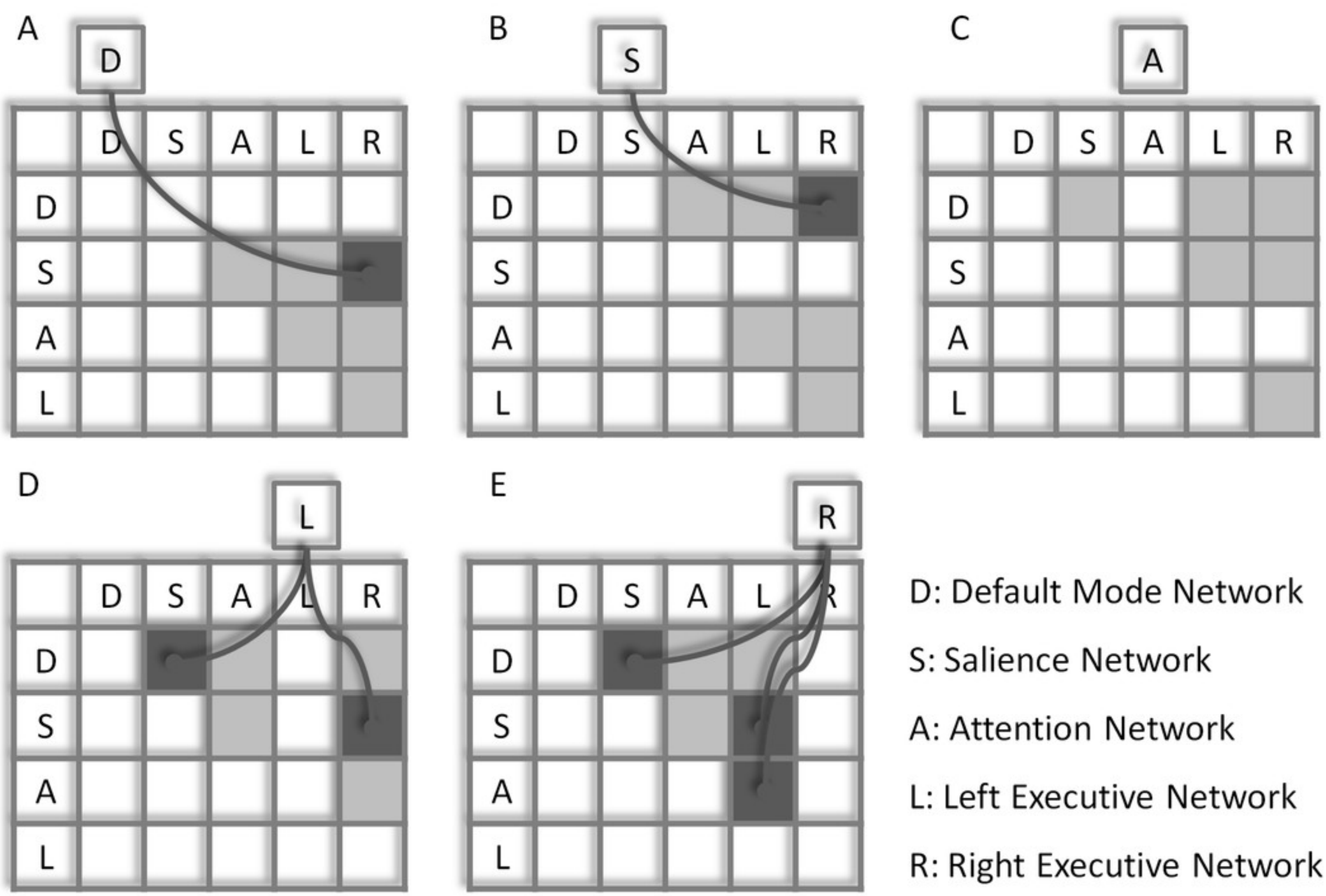

PeerJ PrePrints | https://peerj.com/preprints/124v1/ | v1 received: 27 Nov 2013, published: 27 Nov 2013, doi: 10.7287/peerj.preprints.124v1

Figure 3

PPI results between the DMN and salience network.

Clusters were thresholded at $p < 0.001$ with a cluster level FDR correction at $p < 0.05$. Hot color encodes positive PPI effects, and winter color encodes negative PPI effects. x, y, and z represent x, y, and z coordinates in the MNI space.

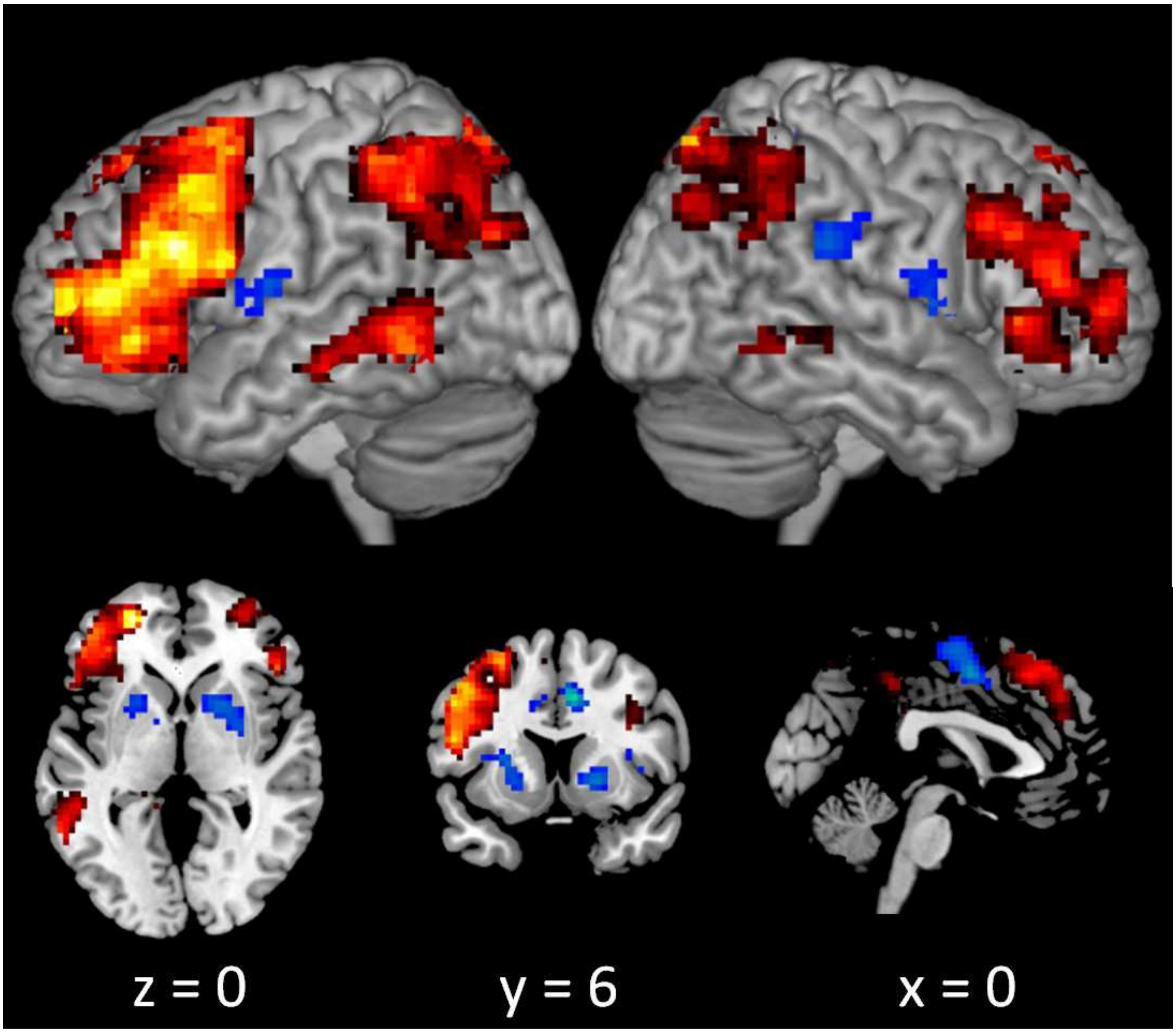

Figure 4

PPI results between the DMN and other task positive networks.

Clusters were thresholded at $p < 0.001$ with a cluster level FDR correction at $p < 0.05$. Hot color encodes positive PPI effects, and winter color encodes negative PPI effects. z represents z coordinates in the MNI space.

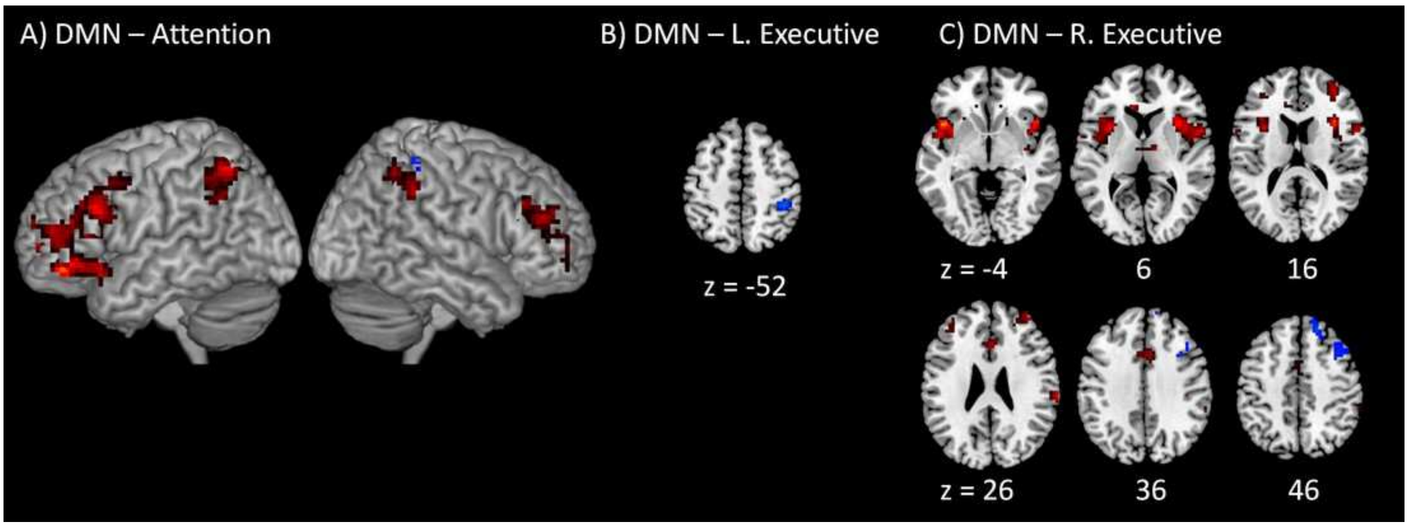

PeerJ PrePrints | https://peerj.com/preprints/124v1/ | v1 received: 27 Nov 2013, published: 27 Nov 2013, doi: 10.7287/peerj.preprints.124v1

Figure 5

PPI results between the salience network and other task positive networks.

Clusters were thresholded at $p < 0.001$ with a cluster level FDR correction at $p < 0.05$. Hot color encodes positive PPI effects, and winter color encodes negative PPI effects. z represents z coordinates in the MNI space.

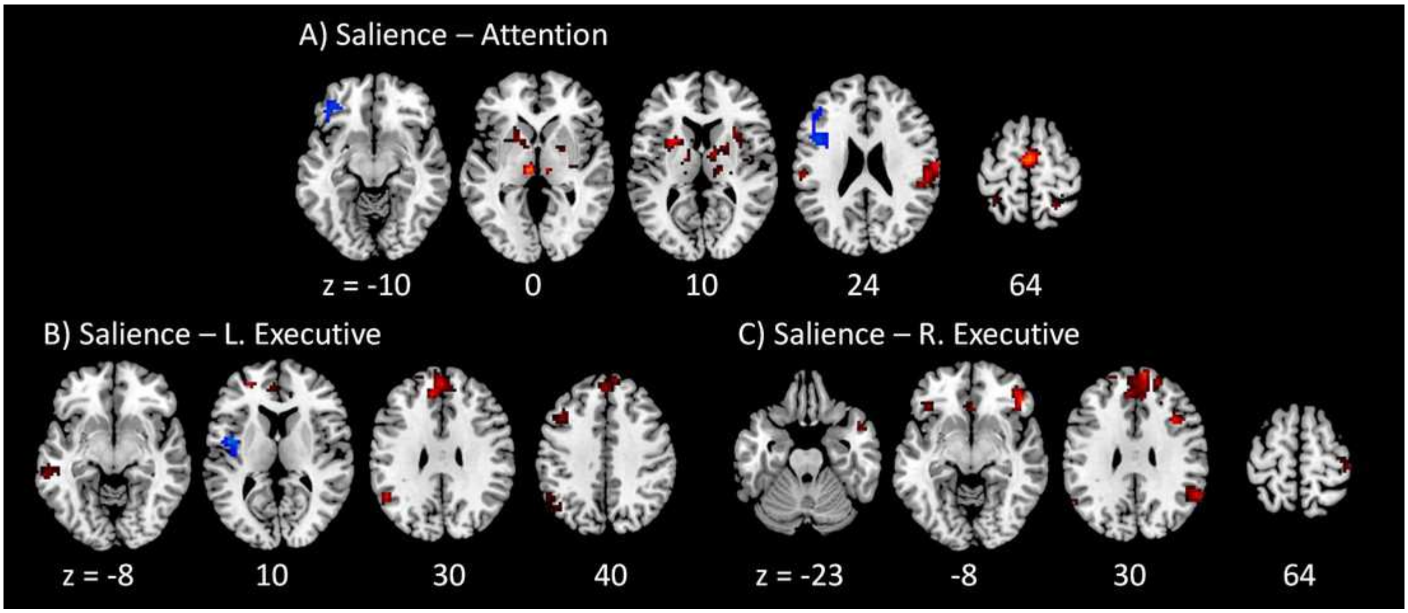

PeerJ PrePrints | https://peerj.com/preprints/124v1/ | v1 received: 27 Nov 2013, published: 27 Nov 2013, doi: 10.7287/peerj.preprints.124v1

Figure 6

PPI results between the dorsal attention and executive networks.

Clusters were thresholded at p < 0.001 with a cluster level FDR correction at p < 0.05. Hot color encodes positive PPI effects, and negative color encodes negative PPI effects. z represents z coordinates in the MNI space.

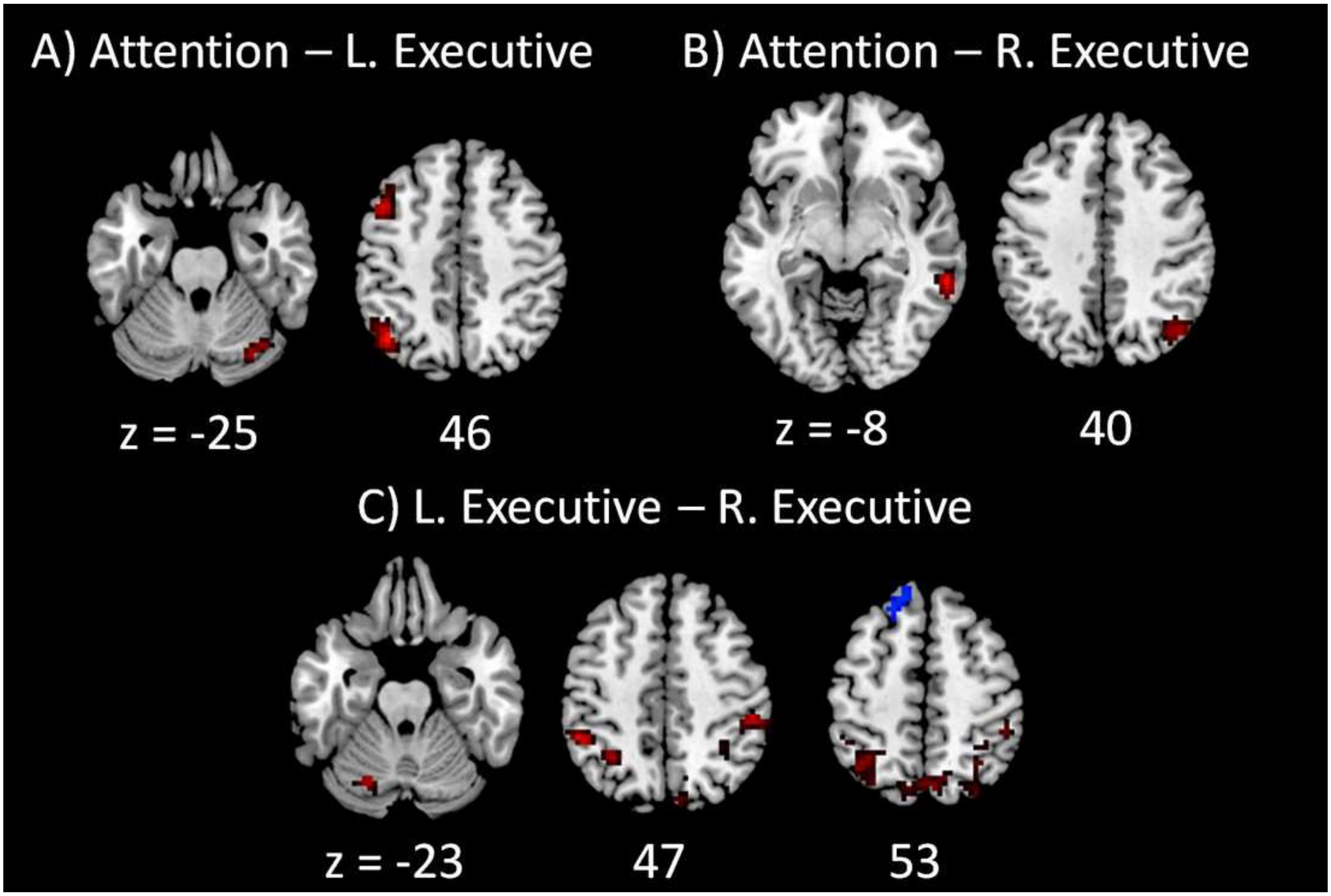

PeerJ PrePrints | https://peerj.com/preprints/124v1/ | v1 received: 27 Nov 2013, published: 27 Nov 2013, doi: 10.7287/peerj.preprints.124v1

Table 1 (on next page)

Mean correlations (Fisher's z scores) among the five networks.

Values in brackets represent p values of corresponding cross subject one sample t-test. Bold font indicates statistically significant.

PeerJ PrePrints | https://peerj.com/preprints/124v1/ | v1 received: 27 Nov 2013, published: 27 Nov 2013, doi: 10.7287/peerj.preprints.124v1

Table 1 Mean correlations (Fisher's z scores) among the five networks. Values in brackets represent p values of corresponding cross subject one sample t-test. Bold font indicates statistically significant.

	DMN	Salience	Attention	L Executive
Salience	**-0.299 (1.34×10^{-16})**			
Attention	**-0.530 (1.55×10^{-28})**	**0.333 (8.45×10^{-16})**		
L Executive	**0.184 (8.25×10^{-10})**	**0.076 (4.06×10^{-3})**	0.003 (0.87)	
R Executive	**0.247 (2.37×10^{-13})**	**-0.142 (1.09×10^{-7})**	0.004 (0.87)	**0.427 (3.83×10^{-28})**

PeerJ PrePrints | https://peerj.com/preprints/124v1/ | v1 received: 27 Nov 2013, published: 27 Nov 2013, doi: 10.7287/peerj.preprints.124v1